
This is an electronic reprint of the original article.
This reprint may differ from the original in pagination and typographic detail.

Völkel, Laura; Rusakov, Dmitrii; Kontturi, Eero; Beaumont, Marco; Rosenau, Thomas;
Potthast, Antje

Manufacturing heat-damaged papers as model materials for evaluating conservation methods

Published in:
Cellulose

DOI:
[10.1007/s10570-022-04657-9](https://doi.org/10.1007/s10570-022-04657-9)

Published: 01/07/2022

Document Version
Publisher's PDF, also known as Version of record

Published under the following license:
CC BY

Please cite the original version:
Völkel, L., Rusakov, D., Kontturi, E., Beaumont, M., Rosenau, T., & Potthast, A. (2022). Manufacturing heat-damaged papers as model materials for evaluating conservation methods. *Cellulose*, 29(11), 6373-6391. <https://doi.org/10.1007/s10570-022-04657-9>

This material is protected by copyright and other intellectual property rights, and duplication or sale of all or part of any of the repository collections is not permitted, except that material may be duplicated by you for your research use or educational purposes in electronic or print form. You must obtain permission for any other use. Electronic or print copies may not be offered, whether for sale or otherwise to anyone who is not an authorised user.



Manufacturing heat-damaged papers as model materials for evaluating conservation methods

Laura Völkel · Dmitrii Rusakov · Eero Kontturi ·
Marco Beaumont · Thomas Rosenau ·
Antje Potthast 

Received: 11 February 2022 / Accepted: 17 May 2022 / Published online: 9 June 2022
© The Author(s) 2022

Abstract Direct fire, indirect heat, and extinguishing water cause great damage to cultural assets upon a fire disaster in a library or archive. Conservation and restoration of heat-damaged papers are particularly challenging due to the complexity and severity of the damage. Since valuable originals obviously cannot be used for the development of treatment methods and only to a limited extent for the analysis of the damage, it is necessary to produce model paper materials that have a high degree of similarity to fire-damaged papers, which was addressed in the present study. Three different heating methods were tested to produce model papers of different heating levels. Their

altered optical, structural, and chemical properties were analyzed and compared with the results of original fire-damaged samples. The study points out pathways to enable the production of comparable sample materials. Heating between hot plates or in an oven produces papers that have properties quite similar to the originals in terms of surface area, paper structure, cellulose integrity, and interactions with water. Stack heating in the oven has proven to be a particularly effective manufacturing method for larger quantities of model papers.

Keywords Paper · Heat-damaged cellulose · Surface structure · Chemical analysis · Heating methods · Thermal aging · Thermal stress

Supplementary Information The online version contains supplementary material available at <https://doi.org/10.1007/s10570-022-04657-9>.

L. Völkel · D. Rusakov · M. Beaumont · T. Rosenau ·
A. Potthast (✉)
Department of Chemistry, Institute of Chemistry
of Renewable Resources, University of Natural
Resources and Life Sciences, Vienna (BOKU),
Konrad-Lorenz-Strasse 24, 3430 Tulln, Austria
e-mail: antje.potthast@boku.ac.at

L. Völkel
Department of Conservation and Special Collections,
Herzogin Anna Amalia Bibliothek/Klassik Stiftung
Weimar, Platz der Demokratie 1, 99423 Weimar, Germany

E. Kontturi
Department of Bioproducts and Biosystems, Aalto
University, P.O. Box 16300, 00076 Aalto, Finland

Introduction

Despite extensive attempts to prevent fire disasters at cultural heritage sites (European Commission. Directorate General for Education, Youth, Sport and Culture 2018), such as museums, libraries, and archives, catastrophic burns do occur regularly and cause severe damage to valuable cultural assets. Recent examples of disasters are the fires in the Brazilian National Museum in Rio de Janeiro in 2018 (Herrberg 2018), the Notre-Dame Cathedral in Paris in 2019 (Tagesschau 2019), and the Shuri Castle in Naha, Japan also in 2019 (Stark 2019). Fires at the Russian Academy of Sciences in St. Petersburg,

Russia in 1988 (Waters 1996), the Duchess Anna Amalia Library in Weimar, Germany in 2004 (Weber et al. 2014) and the Academic Institute for Scientific Information on Social Sciences in Moscow, Russia in 2015 (Weiss 2015) add to this list. In these fires, many paper objects, such as books, handwritings, and manuscripts, have been severely damaged. To ensure that they are not lost forever, they must be treated for conservation and restoration purposes. This is why these events have been and continue to be a matter of concern, scientific research, and conservation endeavors.

A fire disaster is characterized by extremely high temperatures ($> 1000\text{ }^{\circ}\text{C}$), heat-induced gasification, the influence of extinguishing agents, and unpredictable physical forces acting on the building and the objects inside. Individualized paper sheets usually burn completely under such conditions, especially since extreme temperatures, in the range of approx. $750\text{ }^{\circ}\text{C}$, are generated within a very short time (approx. 15 min) above the library shelves (Wassink and Porck 2005). However, thanks to the low thermal conductivity of paper ($k \approx 0.105\text{ Wm}^{-1}\text{ K}^{-1}$) (Morikawa and Hashimoto 1998), there is a chance that in tightly filled library shelves only the outer edge areas of books will be affected by the fire while the central book areas remain largely intact. Nevertheless, the heat influence on the edges of the paper objects is usually so intense that those areas are often completely burned and thus charred or lost (Havermans 2006; Ahn et al. 2018). The fire damage of paper is closely related to the thermal degradation of cellulose, a complex physiochemical process that includes various temperate-dependent chemical reactions, among others dehydration, depolymerization, cross-linking, and aromatization reactions (Tang and Bacon 1964). Intense research on pyrolysis of cellulosic biomass under oxygen-free conditions has led to numerous insights into processes occurring in different temperature ranges and the formed degradation intermediates and products (Fisher et al. 2002; Burhenne et al. 2013; Dumanlı and Windle 2012). However, the thermal effects on cellulose in an accidental fire are rather different from pyrolysis, since the conditions (pressure, temperature, atmosphere, etc.) are obviously not controlled (Dorez et al. 2014).

In a first comprehensive study, Ahn et al. examined the influence of fire on historical books and analyzed the changes at the endogenous level,

especially near the strongly heated edges. Even in charred paper areas, the fibrous structure of the papers was shown to still be preserved. These areas feature a very high carbon content, *i.e.* carbonized cellulose, and polycyclic aromatic hydrocarbons which correlated positively with the heat impact (Ahn et al. 2018). Another study of fire-damaged papers showed that structural and chemical changes initially occurred mainly on the surface and outer edges of the paper. The interior bulk regions of the cellulose were damaged only with increasing heat and exposure time. The charred paper areas were mainly covered with hydrophobic carbon-rich layers, but still contained sites of high surface energy polar groups. Depending on the heat influence and degree of charring, the damaged paper areas exhibited structural changes in the nano and micro range, leading to increased porosity. This caused enhanced water absorption and was thus counteracting and overcompensating the hydrophobic (water-repelling) effect of charring (Völkel et al. 2022). It was also demonstrated that thermal stress not only produced the expected degradation (chain shortening) of polymeric cellulose, but also caused unanticipated crosslinking effects, by thermal cleavage of glycosidic bonds and trans-glycosylation (Hosoya et al. 2014).

All in all, the heat- and fire-induced damage to historical books and papers are severe and complex, increasing the fragility and severely affecting the surface properties in terms of interactions with water and stabilizing materials. This represents a major challenge for restorers. In order to preserve fire-damaged originals, new conservation and restoration methods must be developed, which enable storage and further handling as well as digitization. For this purpose, new coating compositions and application methods must be developed and tested, which evidently poses the need for suitable sample materials. Such sample papers may additionally be of interest for the development of conservational washing and drying methods. The motivation of this work is the preparation of representative, heat-damaged sample material, which can be used to develop and establish new conservation and restoration strategies for fire-damaged objects. The properties of the artificially heat-damaged model papers were compared with original, fire-damaged samples from the burn at the Duchess Anna Amalia Library in Weimar, where a major fire broke out in

the historic library hall on September 02, 2004 (Ahn et al. 2018; Völkel et al. 2022).

Materials and methods

Heat-damaged original papers

Two books, damaged in the fire of the Duchess Anna Amalia Library in Weimar, were selected as sample material, being characteristic examples of paper damaged by fire. The first work is "Cicero's sämtliche Briefe Band 4" by M. Tullius, translated and explained by Christoph Martin Wieland, from 1811. The second book is an edition of "Diplomatisches Archiv für die Zeit- und Staatengeschichte" from the period 1821-1833.

Artificially heated model papers

Two volumes of matching editions from the early nineteenth century were acquired from an antiquarian bookshop as not fire-damaged, comparative material. The samples of "Cicero's sämtliche Briefe Band 4" will be referred to as paper 1 below, and specimens of "Diplomatisches Archiv für die Zeit- und Staatengeschichte" as paper 2.

Like the originals, the model specimens were made of rag paper which historically was handmade from used textiles, i.e., hemp, flax, or nettle fibers. To serve as a writing or printing base, they were surface-sized with gelatin. The resulting paper sheets were printed using the letterpress process and bound into a book. This sample material was subjected to different heating methods with defined parameters (temperature, time, etc.) to study the thermal effects on the paper properties.

Heating methods

Sheets of the antiquarian volumes were used for the production of heat-damaged model papers. The samples of paper 1 and 2 (single sheets or paper stacks) were heated to different temperatures between heating plates (Heidolph MR Hei-Standard,

20–300 °C/800 W), by an household iron (Tefal FV 3840, 80–200 °C/2300 W) or in an oven (Nabertherm LVT 15/11, up to 3000 °C/3500 W).

- (A) Heating between two heating plates: The single paper sheets were placed on a heating plate and covered from above with either a heated iron (test run 1) or a second heated heating plate (test run 2). The heating time was 8 min. The temperature was varied, and different temperature combinations were tested to produce a variety of heat-damaged samples. It was possible to control the temperature of the heating plates from 90 °C to 400 °C by choosing nine heating settings (SI-Fig. S1).
- (B) Heating of single sheets in an oven: The Nabertherm oven was preheated to the target temperature. The individual sample sheets were placed in the oven at three heating levels (100 °C, 200 °C, 300 °C, ± 20 °C) and for different times (30 s, 60 s, 90 s, and 120 s).
- (C) Heating a paper stack in an oven: A stack of about 15–20 sheets, between two ceramic plates, was placed in the oven. Within 45 min the oven was slowly heated to 300 °C and then switched off (SI-Fig. S2). The stack was slowly cooled down to room temperature inside the oven.

During the heating tests, the temperature was monitored with a sensor (sheath thermocouple sensor type K (OMEGA T310)/GTH 1100 digital thermometer, –50 to 1150 °C). After heating, all samples were equilibrated at room humidity, analyzed, and stored under ambient conditions.

SEM analysis

A scanning electron microscope (Apreo VS SEM, Thermo Scientific, Netherlands) was used with triangularly or rectangularly shaped pieces (10–20 mm \times 5–10 mm), fixed to the sample holder using conductive carbon stickers. Silver paint (Acheson Silver DAG 1415 M, Agar Scientific, UK) was applied around the sample edges to increase conductivity before gold sputtering (5–10 nm) using a sputter coater (JEOL JFC-1200, JEOL Ltd, Japan). High-vacuum secondary electron imaging

was performed between 2 and 5 kV, depending on the specimens' surface sensitivity.

Contact angle measurement

The measurements of contact angles were performed on a drop shape analyzer DSA30 with a camera system using Advance software (version 1.41-02, 2014–2016 from Krüss, Hamburg, Germany). The sessile drop method was used, for which 0.2 µl drops were placed on the paper surface. The contact angles on the paper samples were measured with deionized water and *n*-hexane (≥ 95%, Sigma-Aldrich, Chemie GmbH, Munich, Germany) in air. At least 5 measurements were done per sample or sample surface, calculating mean value and standard deviation under exclusion of outliers.

X-ray photoelectron spectroscopy (XPS) analysis

Chemical surface composition was studied by high-resolution X-ray photoelectron spectroscopy (AXIS 165, Kratos Analytical), using monochromatic Al K α irradiation at 100 W, and an in situ reference of pure cellulose (Johansson and Campbell 2004). The C1s binding energy of 286.6 eV for C–O in cellulose was used as the reference value for binding energy corrections (Beamson and Briggs 1992).

GPC measurement and fluorescence labeling of carbonyl groups

The samples were analyzed for carbonyl group content according to the Carbazole-9-Carbonyl-Oxy-Amine (CCOA) method based on Röhrling et al. (2002a and b) and (Potthast et al. 2003). Cellulose analysis was performed with a GPC MALLS fluorescence detection system using *N,N*-dimethylacetamide/LiCl as solvent and eluent, (Chrapava et al. 2003) to obtain the molecular weight distribution (MWD) and the profiles of oxidized carbonyl groups relative to the MWD. *N,N*-Dimethylacetamide (DMAc; CH₃CON(CH₃)₂; ≥ 99%) was obtained from LGC Standards GmbH (Wesel, Germany). Ethanol (CH₃CH₂OH; abs.) and lithium chloride (LiCl, ≥ 99%) were purchased from Sigma-Aldrich (Sigma-Aldrich, Chemie GmbH, Munich, Germany). The relative standard deviation for carbonyl groups and Mw was below 5%. Papers (heated up to 200 °C)

were analyzed, while samples heated at higher temperatures proved to be insoluble.

Attenuated total reflectance infrared (ATR-IR) spectroscopic analysis

The infrared spectra were obtained on a Bruker IR spectrometer (Bruker alpha-P, Germany) equipped with a diamond ATR crystal. Measurements were performed under ambient conditions under the following operating conditions: range of 4000–600 cm⁻¹; resolution of 1 cm⁻¹; number of scans of 4, and at least 3 measurement points per sample were acquired. Samples were analyzed with Spectragryph optical spectroscopy software (F. Menge, Version 1.2.14, 2020, <http://www.ffmpeg2.de/spectragryph/>).

Thermogravimetric analysis (TGA)

TGA was performed under a nitrogen or oxygen atmosphere with a Netzsch TG 209F analyzer. 7.0–8.0 mg were used per sample. The sample was heated from 25 °C to 600 °C at a heating rate of 10 K min⁻¹. For data evaluation, the first-derivative curves were determined. The data was LOWESS-smoothed with a parameter of 0.1.

Thermal imaging

A closed book and an open book were ignited with a Bunsen burner. The open book was cut in half horizontally beforehand. The combustion process was monitored with a thermal imaging camera (Trotec IC 080 LV) and a reflex camera (Samsung NX 10). The images from the thermal imaging camera were evaluated using the Trotec IC Report software (Version 2.6.0 STD).

Results and discussion

Different methods to produce artificially heat-damaged papers were studied (see the material and methods section for the conditions and parameters). The aim was to produce model papers with properties comparable to original samples damaged by fire. We analyzed the produced model papers considering their surfaces and structures, as well as cellulose integrity at different heating stages.

Temperature profiles of a burning book

First, the temperatures involved in book burning and the temperatures that define individual degradation phases were examined. Thermal imaging was used to monitor the burning process. This experiment was conducted with an open rag paper book and hence unlimited air access (Fig. 1I). The temperature increased to 450 °C within 20–30 s, although only a small area of the book was ignited. After less than a minute (40–50 s), the temperature at the sheet edges reached 700 °C and began to curl upwards and char. Due to the low thermal conductivity of paper, the temperatures in non-ignited regions differed significantly, ranging only between 300 to 425 °C. It only took 10 min for the entire book block to burn completely to char and ash.

In addition, a second, this time closed book was ignited. Here, the heat development upon ignition

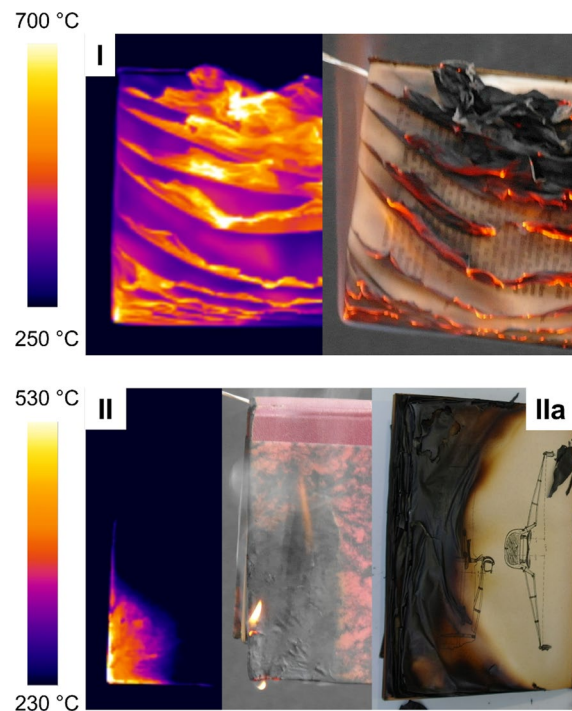


Fig. 1 Combustion experiments and temperature analysis of burning historical rag papers. **I** Due to the unlimited supply of oxygen in the case of an open book, the book pages burn and char entirely and reach higher temperatures of 700 °C. **II** In the closed book scenario, with limited oxygen supply, the temperatures reach lower values with a maximum of 530 °C and the heat-damaged areas are largely restricted to the edges (**IIa**)

occurred mostly occurring at the book edges, as air access to the interior was limited. The burning or glowing edges of the book reached 400 °C to 450 °C at charring (Fig. 1II). The temperatures in the adjacent areas ranged between 230 °C to 400 °C, the maximum temperature and the temperature difference between those regions were smaller than in the case of the open book burning. Ignition took significantly longer, approx. 4 min. This type of heat development, with high temperatures at the edges, narrow temperature gradients, and significantly lower temperatures in the adjacent areas, is also likely to occur upon real fires in libraries, as the volumes are often placed closely adjacent on shelves, which limits the access of air and oxygen to the book interior and individual sheets. Based on these results, we used temperatures ranging from 100 to 400 °C to prepare heat-damaged model samples for the development and testing of stabilization methods.

Combustion phases of rag paper

As shown by thermogravimetric analysis (TGA) in Fig. 2, heating in the presence of oxygen should not exceed 400 °C, otherwise, the thermal degradation is too severe and renders the sample unsuitable for further testing. In presence of oxygen, the degradation (mass loss) of the reference sample occurred in three phases up to its complete decomposition, i.e., combustion to the final products, carbon dioxide and

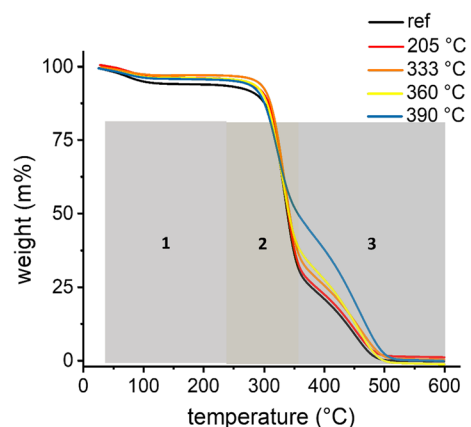


Fig. 2 TGA analysis of heated rag paper samples in air with unlimited oxygen access. Degradation in three phases (labeled as 1–3), which were also observed for pre-heated samples (205 °C, 333 °C, 360 °C, and 390 °C)

◀**Fig. 3** Optical damage patterns resulting from a fire or different heating methods: **I** Paper damage in a library fire: **Ia** typical damage stages—low, medium, and high optical heat damage; **Ib** original damaged sample paper. **II** Heating between heating plates (Method A): **IIa** Samples of heating between an iron and a hot plate, yellow frame: sample heated at 350 °C; **IIb** Samples of heating between two hot plates, yellow frame: sample heated to 392 °C. **III** Heating of single sheets in an oven (Method B): Samples heated at 200 °C (**IIIa**) and at 300 °C (**IIIb**), yellow frame: sample warped significantly. **IV** Heating of stacked paper in an oven (Method C): first (**IVa**) and last (**IVb**) sheet of the stack

dehydration, formation of carbonyl groups, thermal scissions, and gas evolution steps (decarboxylation and decarbonylation) dominate under limited oxygen access, leading to the carbonization of the paper. The underlying chemistry resembles cellulose pyrolysis (Ahn et al. 2018; Tang and Bacon 1964; Dumanlı and Windle 2012; Kawamoto et al. 2003). This stage has the highest mass loss. At unlimited oxygen supply, these reactions are superimposed by typical oxidation reactions, i.e., autocatalytic homolytic (radical) reactions that involve dioxygen and peroxy radicals as the central species. In the third phase from 360 °C to 600 °C, initially formed carbon-rich char decomposes further by oxidative processes and is almost completely converted into gaseous reaction products, mainly CO₂ and water.

Comparing this (reference) TGA profile with preheated samples (Fig. 2), a similar degradation process was observed. Differences were rather minor and dependent on the preheating intensity. In stage 1, physically bound moisture had already escaped during preheating and some chemical water elimination occurred, which is why the mass change is initially lower. Also in stage 2, the mass reduction was lower, and the onset occurred at lower temperatures because partial thermal degradation occurred already during preheating. Similar observations were also made about stage 3. As the preheating allowed the formation and accumulation of relatively stable graphenoid structures, which remained in the paper and were not immediately further consumed in the combustion as in the reference paper, higher temperatures were necessary to completely combust the pre-heated samples (SI-Fig. S3).

In addition, the degradation under a nitrogen atmosphere was studied for comparison (SI-Fig. S4). Due to the lack of oxygen, combustion was incomplete, a stable, graphenoid char resulted, and the

mass reduction of the samples proceeded only in two phases. Generally, elimination and condensation reactions dominate over oxidation reactions which are disfavored by the limited oxygen access. This also changes the dominant reaction types from homolytic (radical) reactions in an air/oxygen atmosphere to heterolytic (ionic, non-radical) processes dominating under nitrogen.

Visual comparison of heat-damaged samples

The original volumes damaged in the fire showed a characteristic damage pattern which is shown in Fig. 3Ia. The edges of the papers were severely damaged by the heat, they were charred, black, fragile and in some cases destroyed. This damage pattern was categorized as “high heat damage”. Gradually transitioning, a brown, heat-damaged area followed, which was defined as “moderate” or “medium heat damage”. This area merged smoothly with the inner area of the sheets, which was visually unaltered and therefore classified as a “low heat damage” region. The individual heat damage pattern is dependent on the extent of fire exposure, i.e., the time and temperature, and varied between samples. This variation is expected: fire causes a complex 3D damage pattern, and within a single book the damage grades between outer and inner book pages usually vary significantly.

In the following, we compare different methods to prepare model papers (methods A, B, and C in Fig. 3), assess the properties of these model papers, and compare them to original paper samples. Heating between hot plates (Method A), heating in an oven as a single sheet (Method B), or heating in an oven in a paper stack (Method C) were used. We previously demonstrated that a purely visual assessment of the damage degree of heat-damaged papers is insufficient (Völkel et al. 2022). The rather subjective evaluation of optical appearance, although still widely used as the basis of conservation decisions, can hardly be regarded as an analytical approach, and must be complemented—if not replaced—with objective and quantifiable data from physicochemical measurements.

When heated plates were used (Method A), the results depended strongly on the equipment used and its heating power. Temperatures of up to 350 °C were achieved either between a heated iron and a heated hotplate or between two heated hotplates (Fig. 3II). It was noticeable that the specimens were heated

unevenly during the tests. Since the iron was not very heavy, the contact between heated surfaces and the paper sheet was not optimal, which caused a non-uniform heat transfer. This led to the formation of lighter and dark charred areas close to each other on the specimen surface (especially at temperatures higher than 300 °C). Only the most heated sample (350 °C) had high optical heat damage (frame in Fig. 3 IIa), the samples heated between 300 °C and 350 °C medium heat damage, and all papers treated at lower temperatures only minor heat damage (see also SI-Fig. S5).

Heating between two heating plates resulted in visually more uniform heat-damaged surfaces. Due to the weight of the plates, their contact with the paper surface was better. In addition, the plates could be heated to higher temperatures of up to 400 °C. Several paper specimens were produced through heating at 361 °C (frame in Fig. 3 IIb), 379 °C, and 392 °C, whereas medium heat damage occurred between 300 °C and 350 °C, and little optical heat damage at lower temperatures (SI-Fig. S6).

The single sheets heated in the oven (Method B) lay freely on a plate and thus had unrestricted contact with the surrounding air (Fig. 3 III). Heating at 200 °C produced uniformly browned, heat-damaged surfaces. They are comparable to the gradual transition between low and medium optical heat damage in originals (Fig. 3 IIIa and SI-Fig. S7). At 300 °C, different degrees of charring are caused at the surface, and the specimens began to warp (Fig. 3 IIIb yellow frame). The paper became very light, thin, and brittle. Comparability with high heat damage in the originals was very good—especially with regard to the charred edges.

However, the unlimited and free access to air during the heating process is very different from the conditions of a real fire in a library, where books are closed and tightly packed together on shelves. Therefore, we also tested Method C, in which a stack of papers was heated between two ceramic plates in the oven, which better simulated the conditions of a closed book (Fig. 3 IV). The temperature of the oven was set to 300 °C and the actual temperature in the center of the paper stack was measured with a temperature sensor. The heat increase in the stack was initially delayed but increased then rapidly to 390 °C, notably exceeding—by far—the set oven temperature of 300 °C (SI-Fig. S2). This effect is caused by the exothermic processes initiated by the heat treatment

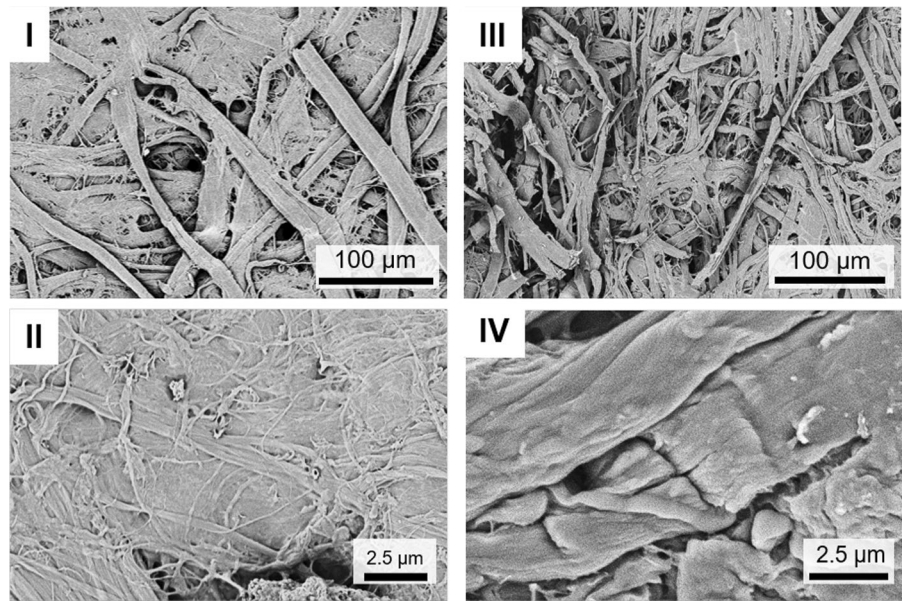
and by the low heat transfer in the paper matrix so that the heat generated is slow to dissipate. The measured temperature in the center of the paper stack does not necessarily have to be the highest temperature occurring. It is likely that many temperature ranges and possibly “hot spots” occur in the stack upon heating due to the low thermal conductivity of paper, which prevents a homogeneous temperature level in the stack.

Method C produced a charred stack of paper with sheets that all corresponded to high heat damage. Nevertheless, the papers exhibited different characteristics depending on their position in the stack. The papers from the upper part of the stack were not completely blackened, but also showed dark brownish spots (Fig. 3 IVa and SI-Fig. S8-I). They were unevenly warped, brittle, fragile, and had completely lost their flexibility. There was no discernible loss of paper thickness. In contrast, the papers from the bottom of the stack were completely black, very thin, light, and brittle, with some remaining flexibility and not as badly warped (Fig. 3 IVb and SI-Fig. S8-II). They had almost completely lost the typical tension of a paper, i.e., any inherent strength in the planar plane was gone, though the paper structure was still held together. Thus, in principle, Method C provided the best comparison to real-world high heat damage. The gradients of different properties from brittle and fragile to thin and very weak made the samples very good mimics of original papers with high to medium heat damage.

Influence of heat on paper structure and wettability

Microscopic examination of original samples (Fig. 4) showed that in the case of low heat damage, the typical paper fiber and network structure with the fibers, small protruding fibrils, and the sizing remained intact and visible (Völkel et al. 2022). Also, in the case of high heat damage, the fiber and network structure were preserved. However, the amount of protruding fibrils and sizing was reduced and broken fiber fragments, as well as cracks, were visible (Ahn et al. 2018; Völkel et al. 2022). Due to the lack of fibrils and sizing, the interstitial spaces increased and at the same time, the fibers shrank, increasing the porosity of the sample. In addition, the surface of individual fibers became smoother due to the intense heat. The fibers appeared fused and smaller fibrils were

Fig. 4 SEM images of surface and fibril structure of the original, heat-damaged paper samples. **I, II** Surface and fiber structure of a paper area with low optical heat damage. **III, IV** Surface and fiber structure of a paper area with high optical heat damage



visible than in the low heat-damaged area (Völkel et al. 2022).

Similar observations were made in the case of the lab-prepared model papers. Figure 5 shows the surface structure of the model papers prepared according to the different methods, comparing the samples with the highest heat damage of each method. Fibrils and sizing residues are still present, but their amount is reduced and cracks on the fibers and their fragments are visible. The fiber diameter was also reduced upon heating, increasing the porosity of the samples. The extent of fiber shrinkage was smaller than in the original specimens, in the order of $A < B < C < \text{original}$ samples (SI-Fig. S9–13). The surface structure of individual fibers (see insets in Fig. 5) was also affected. In the case of individually heated pages (Methods A and B) the fiber surface was significantly smoother and had a fused appearance. In contrast, the fiber surfaces from the upper and lower side of the heated paper staple (Method C) were rougher and similar to non-heated papers.

The discussed surface structures of heat-damaged model papers in comparison to the original papers influence significantly the accessibility of water as well as the bonding of adhesives and stabilizing agents during conservation treatments. It was assumed that due to the charring reactions, the surfaces of the papers have hydrophobic properties, i.e., they are difficult to wet with water. This seemed

logical as progressive charring implies increasing contents of hydrocarbons and graphenoids and thus strongly increased hydrophobicity. This would render water-based restoration measures problematic, as aqueous media would poorly penetrate the surfaces and interact or bind only to a rather limited extent. One method to check hydrophilicity/hydrophobicity is to measure the contact angle. Hydrophobic surfaces have contact angles greater than 90° . If the angle is less than 90° , the surfaces are characterized as hydrophilic. Increasing contact angles with increasing heating impact would indicate enhancement of hydrophobic surface properties.

Due to the structural heterogeneity of rag-paper samples, we used two different samples as noted in the materials section. Paper 1 had a water contact angle of $114 \pm 9^\circ$, i.e., the surfaces were hydrophobic and thus poorly wettable. In contrast, Paper 2 was hydrophilic with a contact angle of $67 \pm 6^\circ$ and thus water-wettable. Differences in hydrophobic or hydrophilic surface properties can be reasoned by a different extent of sizing on the rag papers, which strongly influences the wettability. Sizing, in the production of rag papers, is a step in which papers are surface-coated with animal protein glues (mainly based on gelatin) to render them writable or printable. Gelatin is a film-forming agent and acts as well as an additional protection layer for the rag papers, closing the pores of the paper and smoothing their surface. Upon

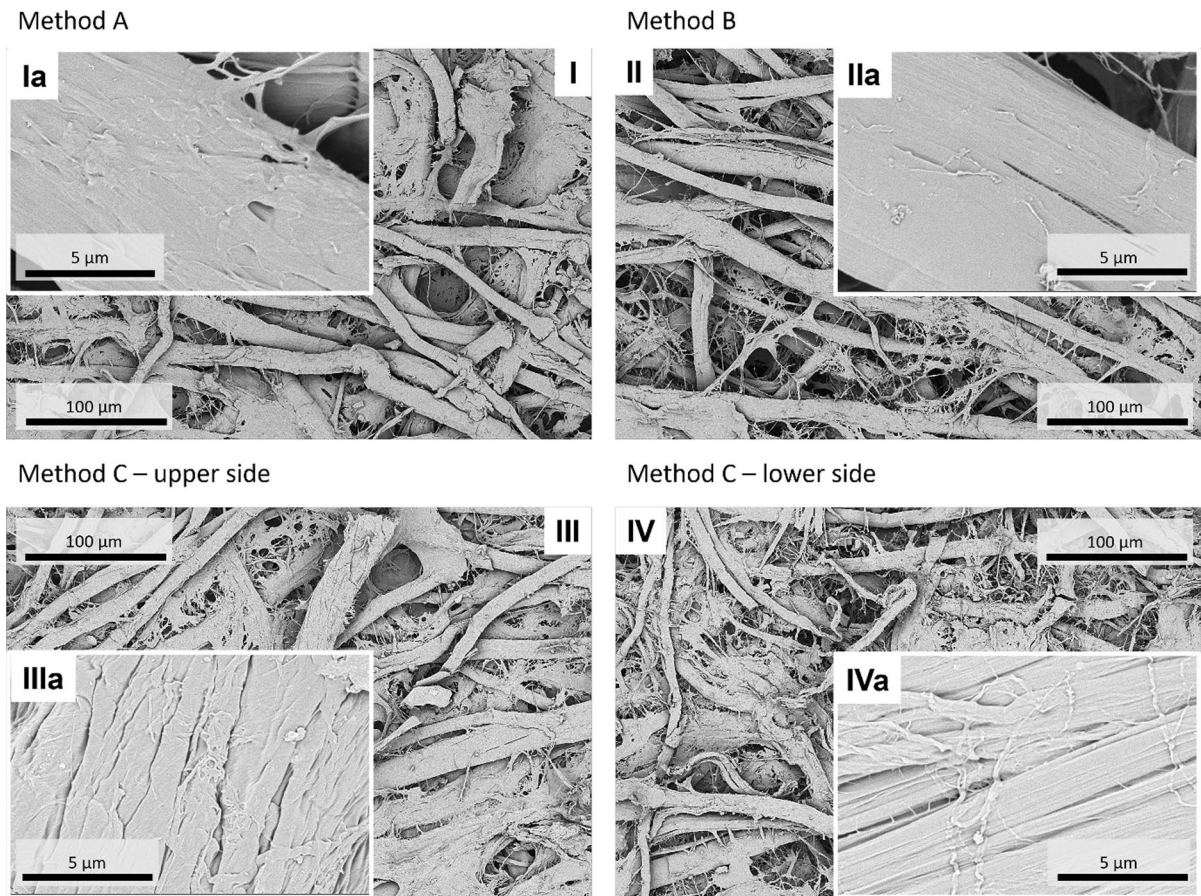


Fig. 5 SEM images of the surface structures of artificially heat-damaged papers at 500 \times and 15,000 \times magnification (insets). **I** Method A—Sample heated up to 392 °C. **II** Method

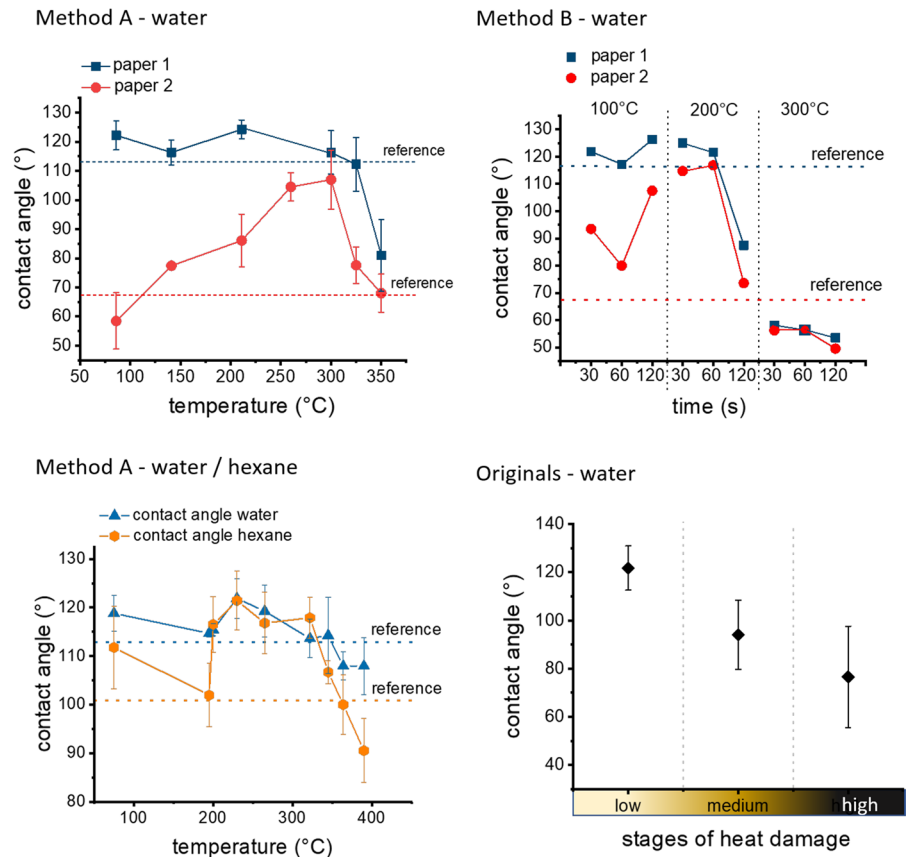
B—Sample heated at 300 °C for 90 s. **III** Method C—First sheet of stack heated to 300 °C. **IV** Method C—Last sheet of stack heated to 300 °C

use and aging of the papers, the gelatin film can be influenced by different factors, which can change the wettability and absorbency of a sized paper (Hunter 1978). Depending on the raw material, the sizing procedure, and the paper manufacturing process, the rag papers are strongly, weakly, or not at all sized, generally spanning over a wide range of surface hydrophilicity/hydrophobicity (Banik and Bruckle 2015).

By producing the model papers with defined temperature effects, we were able to observe for the first time a general stepwise development of the contact angles from their initial state over higher values to lower ones. This allowed a more detailed description and evaluation of their wetting properties. The trend was particularly evident for the samples heated by Method A (Fig. 6).

In the measurement series, the water contact angle initially increased and generally lay above the reference values and above 90° (Fig. 6). Depending on the heating method and paper sample, the temperatures up to which an initial increase was observed varied: up to 300 °C for method A, and up to 200 °C for method B. Progressive dehydration (loss of hydroxyl groups), oxidation of hydroxyl groups to carbonyl groups, and decarboxylation of carboxyl groups render the surface more hydrophobic. This result also correlated with the data from XPS and TGA analysis (see the respective sections for further details). Above these temperatures, the samples in the charred areas showed a rather sudden, significant decrease in contact angle. We also tested the wettability with the nonpolar organic solvent *n*-hexane. Observations were similar to the water case: the contact angle

Fig. 6 Contact angle measurements with water and hexane, comparison of sample papers (heated according to Methods A and B) and the original samples as reference



initially increased and then decreased again at heat exposures above 230 °C. The decrease was even more drastic than with water (Fig. 6).

Considering only the chemical aspect, more charring would increase the content of highly hydrophobic structures (condensed aromatics, graphenoids) and should consequently increase hydrophobicity and the water contact angle. The observed opposite effect was due to the higher porosity of these samples (see above): the surfaces absorbed the liquid droplets quickly like a sponge. The thermal removal of water (physically and chemically) caused the fibers to shrink, in addition, the heat removes sizing agents and degrades fine fibrillar surface structures. These effects significantly increased the porosity of the sample. Above a certain temperature, these physical changes of the surface structure override the effect of the chemical changes resulting in an overall decrease in the contact angle. The physical effects thus overcompensate the chemical impact. The correctness of this interpretation was proven by the fact that for

paper treated at a high temperature of over 300 °C the contact angles of both water and *n*-hexane decreased at the same time. As hydrophilicity and hydrophobicity cannot increase simultaneously, it was evident that the physical porosity effect became dominant, overrunning the influence of surface chemistry.

The important consequence of this observation was that the charred regions of the papers showed good wettability for both polar, especially aqueous, and non-polar solvents.

The complex interplay of physical effects, chemical changes, supply of oxygen and influence on the contact angles was particularly well demonstrated in the case of samples heated in the stack. The uneven heat distribution, but also the limited air supply in the stack, resulted in sample papers with quite different contact angles. For the papers from the upper part of the stack with partly still brownish, partly already black areas, and inflexible, yet preserved paper structure, high water contact angles of $113 \pm 8^\circ$ were measured which were in the range of the reference value.

These values reflect increased surface hydrophobicity in absence of dominant porosity effects. Samples from the lower stacking region with all-black, thin, and heavily altered structures showed a reduced contact angle of $72^\circ (\pm 18^\circ)$, a decrease of 37% compared to the upper paper layers. Now the porosity effects largely dominate. Thus, heating method C simulated the scenario of the fire damage of a closed book quite well, as it properly reflects different extents of damage according to heat and oxygen accessibility.

A similar decrease of the contact angles in the charred, damaged areas has been observed for original papers, although with a more pronounced scattering of the measured values (Völkel et al. 2022). It thus can reasonably be assumed that the course of the contact angles with increasing temperatures (increase followed by decrease) was the same for the original samples. However, due to the greater fire intensity—higher temperatures and longer exposure time—and the close packing of books on library shelves it was

not possible to observe the same stepwise development as in the case of Methods A and B. Only charred areas with high porosity and low contact angles for both polar and non-polar solvents were seen (Völkel et al. 2022). The porous fiber network and the topographic and chemical heterogeneity of the paper which have a high influence on the wettability parameters (contact angle, surface free energy) can also be sources of measurement and interpretation errors (Krolle 2014; Shen et al. 2000).

Heat-induced chemical changes in the paper

The chemical surfaces of samples from Method A and B were examined by X-ray photoelectron spectroscopy (XPS), see Fig. 7. The artificially thermostressed samples had a higher oxygen-to-carbon ratio than the rag paper reference, and the carbon–carbon single bond (C–C) ratios were thus (slightly) reduced. The higher amount of oxygen at the surface indicated

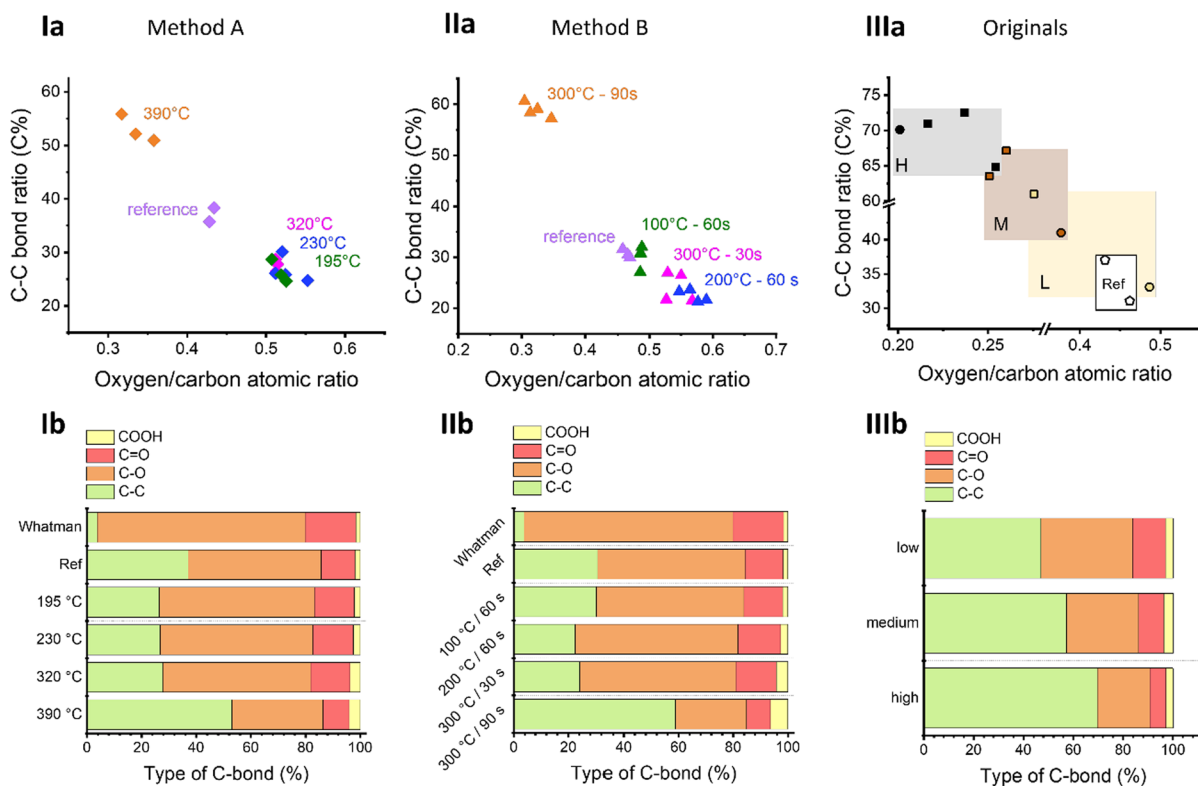


Fig. 7 XPS chemical surface analysis of papers produced according to Method A (**I**), B (**II**), and of the original fire-damaged samples (**III**). The upper row of plots visualizes the

carbon bond content in relation to the oxygen-carbon ratio, the lower row of plots shows the ratio of the different carbon bond types at the sample surfaces

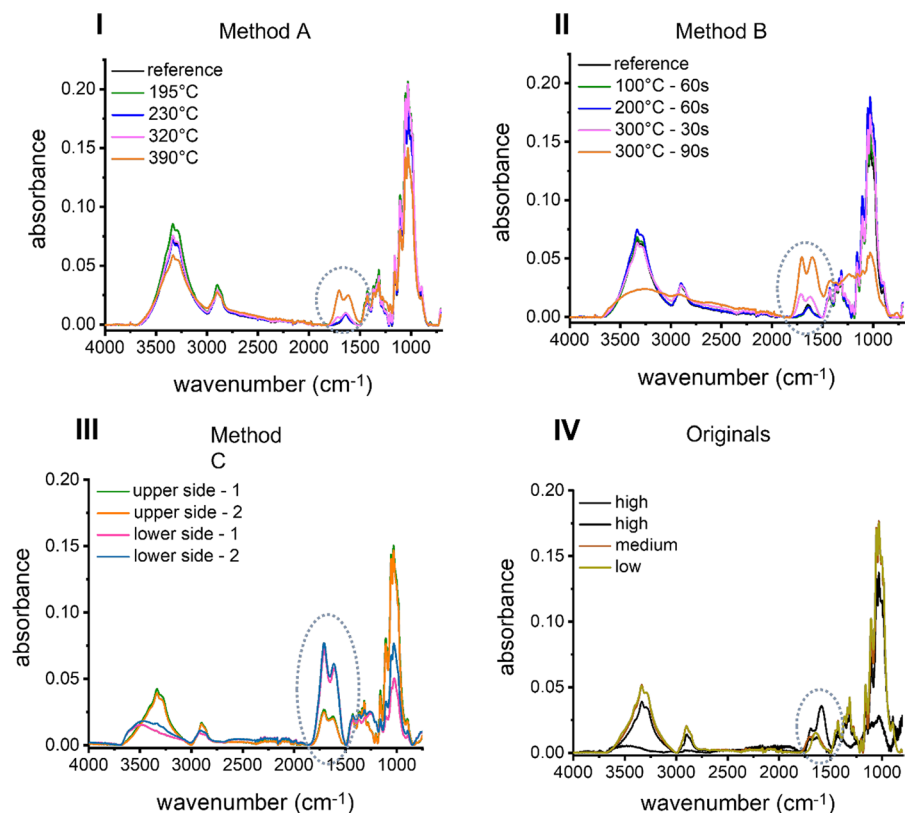
that oxidation reactions (formation of additional carbonyl and carboxyl groups) were still dominant over dehydration and condensation (loss of oxygen) (Fig. 7). This trend was observed for samples from both heating methods. In comparison to Method A, Method B shows a stronger influence of the temperature on the oxygen/carbon ratio, i.e., a wider ratio range, which can be attributed to the larger access of oxygen during heating. The samples heated at 200 °C exhibited the highest oxygen to carbon ratio of the samples, i.e., the highest degree of surface oxygen incorporation. Starting at about 300 °C (Method A 390 °C, Method B 390 °C–90 s), dehydration and condensation cause decreased O/C-ratios through loss of oxygenated volatile compounds. The carbon–carbon single bond content of the samples with the highest heat damage in Method A was about 53% and in Method B 59%, at an oxygen/carbon ratio of only approx. 0.3. These data correlated well with the results from the TGA analysis, which showed a drastic mass decrease starting at 300 °C.

Agreement of the XPS results of model papers and originals (Völkel et al. 2022) was very good.

However, the increase of carbon–carbon single bond ratios and decrease of oxygen/carbon atomic ratios in the artificially heated samples were not as pronounced as in the original papers, since the latter had been exposed to higher temperatures over longer times.

Differences between the properties of the paper surface and the bulk paper can be obtained through a comparison of XPS data and IR spectra, respectively (Völkel et al. 2022). This is due to the varying penetration depth of the two measurement methods. In the XPS measurement, the analysis depth is only a few nm from the material surface, and surface phenomena are measured (Mather 2009). In contrast, the penetration depth of attenuated total reflection IR is in the μm range, which means that also the bulk matrix contributes and heat-induced cellulose degradation beyond surface effects can be observed (Burger et al. 2020; Götz et al. 2020). The combination of these methods showed that thermal effects and charring reactions started as localized processes in nanometer-thin surface regions. Accordingly, the XPS data already showed significant alterations while no changes were yet detectable in the IR spectra (Fig. 8). Only at a

Fig. 8 IR spectra of model papers heated according to methods A (I), B (II), and C (III) in comparison with original samples (IV)



temperature of 300 °C and above, significant changes in the FTIR cellulose spectrum (=in the bulk material) became apparent, whereas the XPS data, C–C single bond ratios, and C/O ratios, started to vary already at lower temperatures starting from 200 °C (=chemical surface changes). This interesting difference between IR and XPS measurements is exemplified in the two IR spectra of the original specimens with high optical heat damage (Fig. 8IV, H1 and H2). Although the XPS spectra indicate high heat damage for both samples H1 and H2, IR reports this damage only in the case of Sample H2 (characteristic cellulose bands being not visible anymore). The difference between these samples can be explained by the different propagation of the heat damage in the paper: in sample H2 the heat damage propagated already further into the bulk matrix of the paper and can hence be detected by IR, whereas in the case of sample H1 heat damage was confined to the immediate (nanoscale) paper surface.

In the IR spectra of heat-damaged model papers prepared at a temperature above 300 °C (Fig. 8 I–III), the intensity of two distinct bands between 1750 and 1550 cm^{-1} increased significantly with the intensity of heat treatment. In the unheated or less heated samples (up to 200 °C), the OH bending band of adsorbed water, which is typical for cellulose samples, dominates at 1630–1640 cm^{-1} . Above 300 °C, new bands appear (the highlighted region in Fig. 8 I–III) indicating the formation of carbonyl groups (corresponding to the band at 1700 cm^{-1}) and conjugated C=C bonds (at 1600 cm^{-1}) due to dehydration/keto-enol and oxidation reactions (Ahn et al. 2018; Tang and Bacon 1964). Longer exposure to temperatures above 400 °C decreases the C=O band and the C=C stretching becomes the dominant band, as observed in the IR spectra of the original samples (Fig. 8IV).

To confirm that these bands are formed due to heat-induced reaction on the cellulose, we compared the IR spectra of a highly pure cellulose sample, Whatman filter paper. This was necessary, to make sure these bands do not correspond, for instance, to amide stretching bands from gelatin or reactions caused by the presence of this protein (sizing agent) (Dumanlı and Windle 2012). We compared the results of pure cellulose and cellulose dipped in gelatin solution beforehand, and got a very similar outcome (SI-Fig. S14): the two stretching bands C=O and C=C described above formed similarly in both samples

when heated to a higher temperature (300 °C). In addition, the intensity of amide IR bands in the gelatin-dipped sample decreased significantly upon heating (SI-Fig. 15). Hence, the gelatin largely decomposes during the charring process and the new bands discussed rather originate from cellulose degradation.

The intensity of the characteristic OH bands around 3300 cm^{-1} and the corresponding C–O band at around 1000 cm^{-1} of the model papers is still significantly higher compared to the original samples with high optical heat damage (Fig. 8IV), which goes hand in hand with previously discussed XPS data results. In general, a decrease of these bands is a result of pronounced charring and loss of oxygenated volatiles. By comparison to literature data on cellulose pyrolysis, we are now able to track the different stages of thermal degradation in the model paper samples and better correlate spectra and observed material damage. Follow-up work is focusing on this special topic. The IR spectra of papers produced with Method C (Fig. 8III) showed again the highest agreement with the original samples, confirming the previous results and demonstrating once more that the degree of damage and charring in original heat-damaged papers can be very well simulated and approached by this method.

Effects on cellulose integrity

The molar mass distribution and the total carbonyl content of celluloses are key factors in the monitoring of damage processes, oxidation, and chain scission caused by the heat. The molecular weight distribution was measured by gel permeation chromatography coupled to multi-angle light scattering, with simultaneous detection of carbonyl groups by group-selective fluorescence labeling (Röhring et al. 2002a; Potthast et al. 2003, 2005, 2015). The effect of the heat damage on the cellulose of original samples has already been discussed in previous works (Ahn et al. 2018; Völkel et al. 2022) and we are now able to correlate those results with the properties of the heat-produced model papers. To follow the progressive thermal degradation and its influence on endogenous levels of the sample, we chose model papers from Method B for GPC analysis. Only analysis of the samples heated to 100 °C and 200 °C, i.e., with low and medium heat damage, was possible (Fig. 9I). The specimens heated to 300 °C and higher could not be analyzed, since

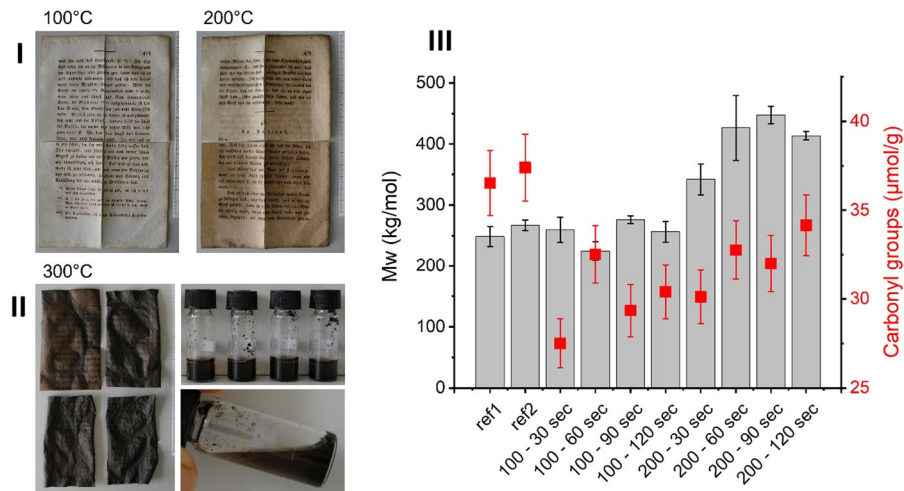


Fig. 9 Heat-induced changes in the bulk matrix of cellulose: **I** analyzed samples heated at 100 °C and 200 °C according to method B. **II** Heating at 300 °C caused the samples to become insoluble and inaccessible for analysis. **III** Molecular weight

(bars) and carbonyl group content (red squares) of the analyzed samples. Error bars of the molecular weight (black): standard deviation of a double determination. Error bars of carbonyl groups (red): standard deviation of 5%

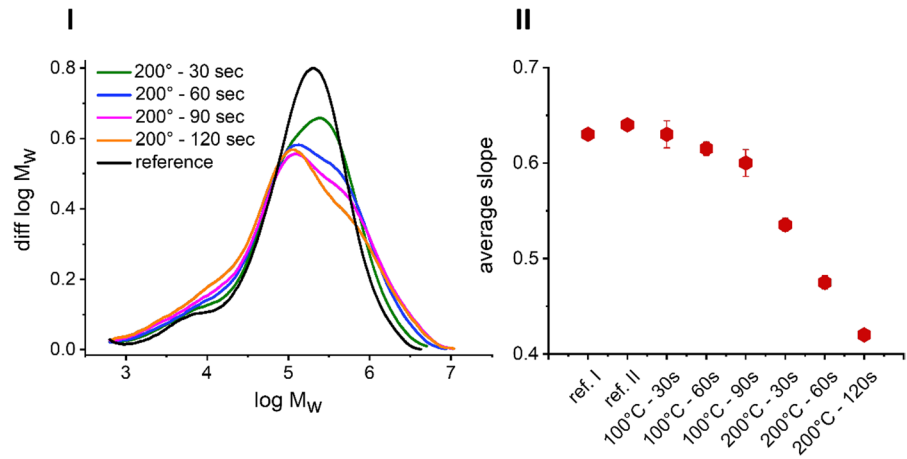
they were insoluble and thus not analytically accessible by the analytical method (Fig. 9II). Similar observations were made also upon analyzing the charred edges of fire-damaged samples (Völkel et al. 2022). This insolubility is caused by extensive crosslinking and condensation as the first stages of far-reaching charring and carbonization.

The analyzable samples provided interesting insights: while one would expect that thermal chain cleavage causes a decrease of the molecular weight, the observed effect was rather the opposite: the average molecular weight (M_w) increased with increasing heat exposure, at least at 200 °C heating temperature (Fig. 9III). This effect is due to cross-linking reactions within the cellulose chains and was also observed in the original samples (Völkel et al. 2022). Oxidized groups, such as carbonyl and carboxyl groups, along the cellulose backbone, serve as reactive crosslinks with neighboring OH groups through (hemi)acetal, (hemi)ketal, and ester formation, respectively, thereby generating both inter- and intra-chain bonds (Ahn et al. 2019). Also, the formation of inter-chain links by non-hydrolyzable carbon–carbon bonds, under the involvement of carbonyl groups as oxidized spots along the cellulose chains, has been reported (Rosenau et al. 2017; Yoneda et al. 2008). This explains also why the number of oxidized groups did not increase significantly despite the oxidizing

conditions. At higher temperatures, also thermal trans-glycosylation reactions set in (Jusner et al. 2022a, 2022b). The resulting crosslinking causes not only an increase in molecular weight but also leads to a densification of the cellulose chains in solution, during GPC measurement, which is seen by analyzing their respective radius of gyration by light scattering (Fig. 10II). A smaller radius in a similar molar mass region points out to a denser polymer chain structure, e.g., due to a higher extent of chemical crosslinking. In the present samples, the crosslinking progressed with heat intensity and is visible through the increasing intensity of the high-molecular-weight shoulder (Fig. 10I). In addition, the decreasing slope of the conformation plot (double logarithmic plot of the radius of gyration vs. molar mass) can be used to estimate the extent of crosslinking (Fig. 10II).

Moreover, also degradation or cleavage of the cellulose chains was observed in the molecular weight distribution profiles (Fig. 10I) through the increase of low-molecular-weight fractions. A rather unusual trimodal distribution was present after heating at 200 °C after 30 s, while the reference sample shows a bimodal distribution. This might indicate an involvement of acids, hydrolytic processes, and trans-glycosidations at elevated temperatures (Hosoya et al. 2014): similar trimodal molar mass distribution patterns are typical of pulps from acidic

Fig. 10 Heat-induced changes in the bulk cellulose. **I** Molecular weight distribution of sample heated to 200 °C according to Method B. **II** Decrease of the slope of the conformation plot (double logarithmic plot of the radius of gyration vs. molar mass) due to crosslinking/aggregation reactions resulting in a denser structure of cellulose molecules in solution



pulping processes. The shortened chains and cellulose fragments appear as wider shoulders in the low-molar mass region. The chain cleavage was also evident in an increased number of reduced end groups with increasing temperature (SI-Fig. S16). Free radical reactions as reported in the literature to occur between 240 °C and 400 °C, should not be major contributors to the heat-induced processes at 100 °C and 200 °C (Tang and Bacon 1964) which occurred in the samples studied by GPC.

The cleavage and the cross-linking of the cellulose are counteracting processes with regard to the molecular weight. They contribute to a significant broadening of the molecular weight distributions as both higher-molecular and low-molecular-weight parts are added (SI-Fig. S17). The processes occurred simultaneously and independently during heating. GPC analysis of the model papers showed the same reaction mechanisms to occur as those previously identified in the original damaged samples (Ahn et al. 2018; Völkel et al. 2022). Thus, the model papers resemble fire-damaged papers very well also on the molecular level which once more corroborates their use in conservation studies.

In summary, the physical and chemical processes during fire damage to paper have the following general characteristics:

- The paper structure becomes porous during the heating process as the fibers shrink and sizing and fibrils are reduced;
- Due to the porosity, aqueous, polar, and non-polar solvents are well absorbed. These physical effects

override the counteracting chemical effect of increased hydrophobicity;

- The charring process starts at the surfaces, which determine interaction with preservation media. Chemical surface alterations can be analytically detected long before those in the bulk material;
- With progressive heating, the proportion of carbon–carbon bonds (C–C and C=C bonds) increases, and the O/C ratio decreases due to the loss of water and oxygenated volatiles, eventually resulting in charring with high contents of graphenoids. The cellulose is progressively altered by simultaneously occurring chain scission and cross-linking processes.

Conclusions

Comprehensive analytical characterization of the produced model papers demonstrated that they have similar properties as original fire-damaged papers with regard to structure, surface, and bulk chemistry as well as molecular cellulose parameters. They are thus very suitable as mimics of fire-damaged papers in conservation studies. The properties of the model papers and the extent of their heat damage depend highly on the respective method and temperature of the treatment.

Method A is a surface-contact heating method, which gives rather heterogeneously damaged samples. At 300–350 °C, very different properties were determined for adjacent regions of the sheet. Dehydration processes and charring are not very pronounced. The

advantage of the method is its simple implementation and the possibility to increase the temperature step by step. The disadvantage is that only one sample can be prepared. This makes the method time-consuming and limits the comparability of produced sample materials. The method does not appear suitable for testing treatment methods in larger quantities and for producing material simulating heavily charred samples.

Method B allows preparing more specimens in a single heating step, the number of samples being limited by the size of the used oven, the plate, and the specimen dimensions. The prepared samples were more uniformly damaged as in the case of Method A. The gradual increase in temperature and heating time also allowed for better controlling the extent of heat damage. The heated specimens showed good comparability with original fire-damaged papers, which is a clear advantage. A drawback is that single papers are heated in this method. As a result, the accessibility and supply of air (oxygen) during heating is rather different from the situation of a real fire at a library, mostly with closed books aligned on shelves. In addition, the produced samples were not flat but wrinkled.

Method C, which is closer to a real library fire, heats a paper stack between two ceramic plates to simulate the conditions in a closed book. This method turned out to be the most promising one, clearly recommendable for the production of heat-damaged model papers. The advantages are that homogeneously heated specimens can be produced, which are very well comparable to severely fire-damaged papers. Due to the stack setup, many samples are produced at once, and the heat gradient effects are similar to the case of an originally fire-damaged book. The heat damage propagates from the side of the stack with the highest air and oxygen accessibility, similar to books on a shelf during the burn. All in all, this method mimics the fire-heating of closed books very well.

The model papers proved very helpful in exercising analytical characterization methods for heated and charred papers since with these specimens larger sample amounts produced under known heating conditions became available. For the first time, it was possible to follow and interpret the individual stages of a rag paper combustion and, at the same time, to confirm that the sample papers were well mimicking their original counterparts. All heating methods can

be performed in conservators' workshops, allowing the preparation of model papers tailored to specific application cases.

Acknowledgments We thank Dr. Leena-Sisko Johansson, Aalto University, Department of Bioproducts and Biosystems, for her support in XPS analysis. For their practical support in the laboratory, we thank Dr. Sonja Schiehser and Paul Jusner. L.V. would like to thank Klassik Stiftung Weimar and the doctoral school ABC&M for financial support. The financial support of the Austrian Biorefinery Center Tulln (ABCT) is also gratefully acknowledged.

Author contributions LV and DR performed the measurements. AP supervised the project. LV, MB AP, EK, TR analyzed the data. LV, MB, and TR wrote and revised the manuscript. All authors read and approved the final manuscript.

Funding Open access funding provided by University of Natural Resources and Life Sciences Vienna (BOKU). The authors acknowledge the financial support from the County of Lower Austria within the framework of the Austrian Biorefinery Center Tulln (ABCT), and the Austrian Science Fund (J4356). The research in this article was conducted within the framework of the doctorate school "Advanced Biorefineries Chemistry and Materials"—ABC&M (LV). L.V. also thanks Klassik Stiftung Weimar for financial support.

Data availability Data available from the corresponding author upon request.

Code availability Not applicable.

Declarations

Conflict of interest None.

Ethical approval Not applicable.

Consent to participate Not applicable.

Consent for publication All authors agreed to the publication in the submitted form.

Open Access This article is licensed under a Creative Commons Attribution 4.0 International License, which permits use, sharing, adaptation, distribution and reproduction in any medium or format, as long as you give appropriate credit to the original author(s) and the source, provide a link to the Creative Commons licence, and indicate if changes were made. The images or other third party material in this article are included in the article's Creative Commons licence, unless indicated otherwise in a credit line to the material. If material is not included in the article's Creative Commons licence and your intended use is not permitted by statutory regulation or exceeds the permitted use, you will need to obtain permission directly from the copyright holder. To view a copy of this licence, visit <http://creativecommons.org/licenses/by/4.0/>.

References

- Ahn K, Schedl A, Zweckmair T, Rosenau T, Potthast A (2018) Fire-induced structural changes and long-term stability of burned historical rag papers. *Sci Rep* 8(1):12036. <https://doi.org/10.1038/s41598-018-30424-7>
- Ahn K, Zaccaron S, Zwirchmayr NS, Hettegger H, Hofinger A, Bacher M, Henniges U, Hosoya T, Potthast A, Rosenau T (2019) Yellowing and brightness reversion of celluloses: CO or COOH, who is the culprit? *Cellulose* 26(1):429–444. <https://doi.org/10.1007/s10570-018-2200-x>
- Banik G, Brückle I (2015) *Papier und Wasser: ein Lehrbuch für Restauratoren, Konservierungswissenschaftler und Papiermacher*, 1st edn. Verlag Anton Siegl Fachbuchhandlung GmbH, München
- Beamson G, Briggs D (1992) High resolution XPS of organic polymers: The scienta ESCA300 database. Wiley, Chichester [Engalnd], New York
- Burger D, Beaumont M, Rosenau T, Tamada Y (2020) Porous silk fibroin/cellulose hydrogels for bone tissue engineering via a novel combined process based on sequential regeneration and porogen leaching. *Molecules* 25(21):5097. <https://doi.org/10.3390/molecules25215097>
- Burhenne L, Messmer J, Aicher T, Laborie M-P (2013) The effect of the biomass components lignin, cellulose and hemicellulose on TGA and fixed bed pyrolysis. *J Anal Appl Pyrol* 101(May):177–184. <https://doi.org/10.1016/j.jaap.2013.01.012>
- Chrapava S, Touraud D, Rosenau T, Potthast A, Kunz W (2003) The investigation of the influence of water and temperature on the LiCl/DMAc/cellulose system. *Phys Chem Chem Phys* 5(9):1842–1847. <https://doi.org/10.1039/B212665F>
- European Commission. Directorate General for Education, Youth, Sport and Culture (2018) Safeguarding cultural heritage from natural and man-made disasters: a comparative analysis of risk management in the EU. Publications Office, LU
- Dorez G, Ferry L, Sonnier R, Taguet A, Lopez-Cuesta J-M (2014) Effect of cellulose, hemicellulose and lignin contents on pyrolysis and combustion of natural fibers. *J Anal Appl Pyrol* 107(May):323–331. <https://doi.org/10.1016/j.jaap.2014.03.017>
- Dumanlı AG, Windle AH (2012) Carbon fibres from cellulosic precursors: a review. *J Mater Sci* 47(10):4236–4250. <https://doi.org/10.1007/s10853-011-6081-8>
- Fisher T, Hajaligol M, Waymack B, Kellogg D (2002) Pyrolysis behavior and kinetics of biomass derived materials. *J Anal Appl Pyrol* 62(2):331–349. [https://doi.org/10.1016/S0165-2370\(01\)00129-2](https://doi.org/10.1016/S0165-2370(01)00129-2)
- Götz A, Nikzad-Langerodi R, Staedler Y, Bellaire A, Saukel J (2020) Apparent penetration depth in attenuated total reflection fourier-transform infrared (ATR-FTIR) spectroscopy of *Allium Cepa* L. epidermis and cuticle. *Spectrochim Acta A: Mol Biomol Spectrosc* 224(January):117460. <https://doi.org/10.1016/j.saa.2019.117460>
- Havermans, John BGA (2006) Paper materials after fire. Degradation, mould and emission. *PapierRestaurierung* 7(2):31–34
- Herrberg A (2018) “Katastrophe Für Die Kultur Brasiliens. Brand Im Nationalmuseum in Rio de Janeiro.” *Deutschlandfunk*, September 3, 2018. https://www.deutschlandfunk.de/brand-im-nationalmuseum-in-rio-de-janeiro-katastrophe-fuer.691.de.html?dram:article_id=427143;21.01.2021.
- Hosoya T, Takano T, Kosma P, Rosenau T (2014) Theoretical foundation for the presence of oxocarbenium ions in chemical glycoside synthesis. *J Org Chem* 79(17):7889–7894. <https://doi.org/10.1021/jo501012s>
- Hunter D (1978) *Papermaking: the history and technique of an ancient craft*. Dover Publications, New York
- Johansson L-S, Campbell JM (2004) Reproducible XPS on biopolymers: cellulose studies. *Surf Interface Anal* 36(8):1018–1022. <https://doi.org/10.1002/sia.1827>
- Jusner P, Bacher M, Simon J, Bausch F, Khaliliyan H, Schiehser S, Sumerskii I, Schwaiger E, Potthast A, Rosenau T (2022a) Analyzing the effects of thermal stress on insulator papers by solid-state ¹³C NMR spectroscopy. *Cellulose* 29(2):1081–1095. <https://doi.org/10.1007/s10570-021-04338-z>
- Jusner P, Bausch F, Schiehser S, Schwaiger E, Potthast A, Rosenau T (2022b) Protocol for characterizing the molar mass distribution and oxidized functionality profiles of aged transformer papers by gel permeation chromatography (GPC). *Cellulose* 29(4):2241–2256. <https://doi.org/10.1007/s10570-022-04464-2>
- Kawamoto H, Murayama M, Saka S (2003) Pyrolysis behavior of levoglucosan as an intermediate in cellulose pyrolysis: polymerization into polysaccharide as a key reaction to carbonized product formation. *J Wood Sci* 49(5):469–473. <https://doi.org/10.1007/s10086-002-0487-5>
- Krolle A (2014) “Benetzbarkeit der Papieroberfläche. Charakterisierung der Papieroberfläche für nachfolgende Verarbeitungsprozesse.” Dissertation, Graz: Technische Universität Graz. <https://diglib.tugraz.at/download.php?id=58dc335184ab6&location=browse>. Accessed 20 Apr 2021.
- Mather RR (2009) 13—Surface modification of textiles by plasma treatments. In: Wei Q (ed) *Surface modification of textiles*. Woodhead Publishing Series in Textiles, Woodhead Publishing, Sawston, pp 296–317. <https://doi.org/10.1533/9781845696689.296>
- Morikawa J, Hashimoto T (1998) Thermal diffusivity measurement of papers by an Ac Joule heating method. *Polym Int* 45(2):207–210. [https://doi.org/10.1002/\(SICI\)1097-0126\(199802\)45:2%3c207::AID-PI894%3e3.0.CO;2-Y](https://doi.org/10.1002/(SICI)1097-0126(199802)45:2%3c207::AID-PI894%3e3.0.CO;2-Y)
- Potthast A, Röhring J, Rosenau T, Borgards A, Sixta H, Kosma P (2003) A novel method for the determination of carbonyl groups in celluloses by fluorescence labeling. 3. Monitoring oxidative processes. *Biomacromol* 4(3):743–749. <https://doi.org/10.1021/bm025759c>
- Potthast A, Rosenau T, Kosma P, Saariaho A-M, Vuorinen T (2005) On the nature of carbonyl groups in cellulosic pulps. *Cellulose* 12(1):43–50. <https://doi.org/10.1023/B:CELL.0000049347.01147.3d>
- Potthast A, Radosta S, Saake B, Lebioda S, Heinze T, Henniges U, Isogai A, Koschella A, Kosma P, Rosenau T, Schiehser S, Sixta H, Strlič M, Strobin G, Vorwerg W, Wetzel H (2015) Comparison testing of methods for gel

- permeation chromatography of cellulose: coming closer to a standard protocol. *Cellulose* 22(3):1591–1613. <https://doi.org/10.1007/s10570-015-0586-2>
- Röhring J, Potthast A, Rosenau T, Lange T, Borgards A, Sixta H, Kosma P (2002a) A novel method for the determination of carbonyl groups in celluloses by fluorescence labeling. 2. Validation and applications. *Biomacromol* 3(5):969–975. <https://doi.org/10.1021/bm020030p>
- Röhring J, Potthast A, Rosenau T, Lange T, Ebner G, Sixta H, Kosma P (2002b) A novel method for the determination of carbonyl groups in celluloses by fluorescence labeling. 1. Method development. *Biomacromol* 3(5):959–968. <https://doi.org/10.1021/bm020029q>
- Rosenau T, Potthast A, Kosma P, Hosoya T, Henniges U, Mereiter K, French AD (2017) 2,4':2',4 Dianhydride of 3-ketoglucoside, a precursor to chromophores of aged, yellow cellulose, and its weak interactions. *Cellulose* 24(3):1227–1234. <https://doi.org/10.1007/s10570-017-1198-9>
- Shen W, Filonanko Y, Truong Y, Parker IH, Brack N, Pigram P, Liesegang J (2000) Contact angle measurement and surface energetics of sized and unsized paper. *Colloids Surf, A* 173(1):117–126. [https://doi.org/10.1016/S0927-7757\(00\)00454-4](https://doi.org/10.1016/S0927-7757(00)00454-4)
- Stark F (2019) “Großfeuer Zerstört Die Burg Der ‘Musterbarbaren.’” *Welt*, October 31, 2019. <https://www.welt.de/geschichte/article202775138/Weltkulturerbe-Okina-wa-Grossfeuer-zerstuert-Burg-der-Musterbarbaren.html> Accessed 21 Jan 2021.
- Tagesschau. 2019. “Feuer in Pariser Kathedrale. Brand in Notre-Dame Unter Kontrolle.” *Tagesschau*, April 16, 2019. <https://www.tagesschau.de/ausland/notre-dame-155.html> Accessed 21 Jan 2021.
- Tang MM, Bacon R (1964) Carbonization of cellulose fibers—I. Low temperature pyrolysis. *Carbon* 2(3):211–220. [https://doi.org/10.1016/0008-6223\(64\)90035-1](https://doi.org/10.1016/0008-6223(64)90035-1)
- Völkel L, Beaumont M, Johansson L-S, Czibula C, Rusakov D, Mautner A, Teichert C, Kontturi E, Rosenau T, Potthast A (2022) Assessing fire-damage in historical papers and alleviating damage with soft cellulose nanofibers. *Small*. <https://doi.org/10.1002/sml.202105420>
- Wassink B, and Porck HJ (2005) “Boeken in brand—de Gevolgen van Brandschade Voor Het Papieren Erfgoed/Burning Books—the consequences of fire damage to the paper heritage,” 198–215.
- Waters P (1996) From florence to St. Petersburg: an enlightening and thought-provoking experience. A personal account of the past twenty nine years in pursuit of the conservation of library materials. *Redefining disasters: A decade of counter-disaster planning*. State Library of New South Wales, Sydney, pp 237–49
- Weber J, Hähner U eds (2014) *Restaurieren nach dem Brand: die Rettung der Bücher der Herzogin Anna Amalia Bibliothek*. Petersberg: Imhof.
- Weiss C (2015) “Catastrophic Fire at Russia’s Most important social science library.” *International Committee of the Fourth International (ICFI)*. <https://www.wsws.org/en/articles/2015/02/10/russ-f10.html>. Accessed 10 Feb 2015
- Yoneda Y, Mereiter K, Jaeger C, Brecker L, Kosma P, Rosenau T, French A (2008) Van Der Waals versus hydrogen-bonding forces in a crystalline analog of cellotetraose: cyclohexyl 4'-O-cyclohexyl β -d-cellobioside cyclohexane solvate. *J Am Chem Soc* 130(49):16678–16690. <https://doi.org/10.1021/ja805147t>

Publisher’s Note Springer Nature remains neutral with regard to jurisdictional claims in published maps and institutional affiliations.